Journal of Solid Mechanics Vol. 12, No. 2 (2020) pp. 249-262
DOI: 10.22034/jsm.2020.672978

A Novel Finite-Element-Based Algorithm for Damage Detection in the Pressure Vessels Using the Wavelet Approach

N. Haghshenas[1], A.H. Ghorbanpour Arani [1] , A. Javanbakht [2], M. Karimi [3,*]

[1]*School of Mechanical Engineering, College of Engineering, University of Tehran, Tehran, Iran*
[2]*Faculty of Mechanical Engineering, University of Kashan, Kashan, Iran*
[3]*Engineering Faculty, Mechanical Engineering Department, Bu Ali Sina University, Hamedan, Iran*

Received 19 January 2020; accepted 22 March 2020

ABSTRACT

In this investigation, a suitable algorithm for the detection of cracks in the pressure vessels is presented. The equations of motion for the vessel are obtained and transferred into the wavelet space in a simplified form resulted from time and position approximations. The locations of cracks are randomly distributed in different regions of the structure to cover the whole geometry of the pressure vessel. Furthermore, the pressure vessel is installed vertically with a fixed end at the bottom of each of its four leg supports. Then, the results are transferred to the wavelet space using Daubechies wavelet families. From the comparison of the displacement results associated with the intact and damaged vessels, it can be clearly seen that the crack location can be accurately detected noting the alteration in the wavelet output diagrams .The results of the crack detection show that with the proper selection of the wavelet type, the wavelet based finite element method is a suitable and nondestructive method as well as a powerful numerical tool for the detection of cracks and other discontinuities in the pressure vessels. The results of this investigation can be used in the marine and aerospace industries as well as power stations.

Keywords: Crack detection, Pressure vessel, Cylindrical vessel, Wavelet method, Daubechies wavelet.

1 INTRODUCTION

STRUCTURAL health and identifications of defects associated with steel structures are important problems in the industry. Crack growth is a crucial factor that can result in the structure failure and, therefore, should be considered as a destructive factor regarding the structural integrity. Various methods are presented in the literature in order to address the practical issue of Damage detection in the structures that is of crucial importance in the industry. Gudmaunsom [1] used turbulence method for the identification of changes in the natural frequencies of the

*Corresponding author. Tel.: +98 813 8292505-8 ; Fax: +98 813 8292631.
E-mail address: karimi_mh@yahoo.com (M. Karimi).

structures due to cracks showing that Damage can lead to changes in the mechanical properties of the structure. According to the mechanical principles of the structural theory, the static and dynamic response of a structure is related to its stiffness. Any sort of changes in the stiffness of the structure will be accompanied by changes in the static and dynamic response. By investigating the response of structures, one can determine the characteristics of defects [2]. Dynamic systems are dependent on vibration mode shapes that are obtained by physical properties and space distributions. Prediction of response of a structure to vibrations or external loadings, have many applications. This prediction is done based on an exact mathematical model that can be obtained by modal analysis. Modal analysis as a nondestructive and useful test gives valuable information about the degree of safety of structures and economic decisions related to them [3]. One of the first studies about crack detection using wavelet method have been done by Li et al [4]. Another study about determining specification of damage have been done Samii and Lotfi [5] in which they present a method based on wavelet finite element. Douka et al [6] investigated diagnosis of the location and depth of crack in cantilever beams by using wavelet transform. Bagheri et al [7,8] presented a method by using 2D discrete wavelet transform for detecting damage in plates. Rizos et al [9] offered a way from measurement range in tow point of a cantilever beam that vibrates in one of the natural modes. In addition, an exact comparison between the two methods –natural based and mode shape based– for detecting damage in beam structures are released by Kim and Melhem [10]. One of the common points in all researches is that the methods are more sensitive to changes in mode shapes rather than in natural frequencies. Ovanesova and Suarez [11] studied a beam subjected to static and dynamic loads using different discrete and continuous wavelet transform. The proposed method is based on the assumption that the structural damage cause disorder in the structural response. Although this disorder may not be recognizable in the direct study of structure response but by establishing the continuous wavelet transform coefficients or partial signal of discrete wavelet transform, lack of uniformity of the signal can be identified. The results show that the location of crack can be identified with high accuracy. Khatam and Golafshani [12] showed that it is impossible to detect the damage in intact and damaged beam using Fourier spectrum and it requires a tool that locate the propellant of small changing in signal frequency content. Cawely and Adams [13] used an experimental method from changing in natural frequencies for locating crack and finding its depth. Gokdag and Kompaz [14] successfully detected damage in beams by compound discrete and continuous wavelet transformation. In this method, mode shapes of damaged structures have been considered as a combination of mode shapes of intact structures and factors such as error due to measurement and local damage. Rucka [15] investigated the effect of mode orders on ability of damage detecting in structures. For the detection of damage, he used continuous wavelet transform of normalized mode shapes. For this purpose, he studied the numerical and experimental analysis of eight modes of a cantilever beam. At the end, he found out that the higher the order of mode shapes, the higher the chance of achieving a reliable result which overall indicates higher mode sensitivity. As an extension of wavelet based crack detection concept to the laminated structures, Tao et al [16] studied the dynamic responses of cracked fiber metal laminated (FML) beams under the action of a moving load using the modal expansion theory and Newmark method. They employed continuous wavelet transform (CWT) for the crack detection in the Euler-Bernoli FML beam and showed that various parameters such as crack depth and crack location as well as ply angle of the fiber layer have significant effect on the free and forced vibration of the FML beam. In a more recent experimental investigation Mardasi et al [17] developed an optimized wavelet analysis performed on a deflected aluminum cantilever beam. They introduced optimized scale factors into the Gabor wavelet transformation scheme and employed the windowing functions in order to address the issue of wavelet edge effect that arises around the boundaries of measured data. They showed the aforementioned spatial wavelet analysis is highly sensitive even to the small cracks with a size less than 10% of the beam height.

In this paper, the cylindrical pressure vessel and cracks with proper definition of mesh regions are modeled in the Abaqus software. Then, the results are transferred into Matlab software for further wavelet analysis. The overall procedure presented in this investigation can be reconstructed in the same manner for other specific problems with regard to the detection of any type of structural damage specially cracks in the structures including cylindrical shell parts such as pressure vessels.

2 CYLINDRICAL COORDINATE SYSTEM

Considering the geometry of the vessel, cylindrical coordinate system with three coordinates z, θ, and r is employed and the governing differential equations are derived based on the symmetrical displacement assumption with respect to the circumferential direction. As a result, only the axial and radial displacements are included in these equations, which can be denoted, by w and u, respectively.

Therefore, one can show that the equation of motion corresponding to the radial direction for the isotropic cylindrical vessel can be written as:

$$(\lambda+2\mu)\nabla_0^2\Delta=\rho\frac{\partial^2\Delta}{\partial t^2} \tag{1}$$

On the other hand, in the simple form as:

$$c_d^2\nabla_0^2\Delta=\frac{\partial^2\Delta}{\partial t^2} \tag{2}$$

where ∇_0^2 is an operator acting on the variable Δ which will be defined shortly, λ,μ are Lame constants, ρ is density, t is time, and c_d is a constant which can be calculated as:

$$c_d^2=(\lambda+2\mu)/\rho \tag{3}$$

In addition, the second equation of motion with respect to the circumferential direction can be expressed as:

$$\mu\nabla_1^2\mho_\theta=\rho\frac{\partial^2\mho_\theta}{\partial t^2} \tag{4}$$

Alternatively, in the general form as:

$$c_S^2\nabla_1^2\mho_\theta=\frac{\partial^2\mho_\theta}{\partial t^2} \tag{5}$$

where c_s is simply expressed as:

$$c_S^2=\mu/\rho \tag{6}$$

Moreover, $\nabla_n^2\ (n=0,1)$ can be written as:

$$\nabla_n^2\equiv\frac{\partial^2}{\partial r^2}+\frac{1}{r}\frac{\partial}{\partial r}-\frac{n^2}{r^2}+\frac{\partial^2}{\partial z^2} \tag{7}$$

which represent operators acting on $\Delta,\mho_\theta$ denoting the generalized radial and circumferential strain components [15], respectively, with defining expressions as:

$$\Delta=\frac{1}{r}\frac{\partial(ru)}{\partial r}+\frac{\partial\omega}{\partial z} \tag{8}$$

$$\mho_\theta=\frac{\partial u}{\partial z}+\frac{\partial\omega}{\partial r} \tag{9}$$

with simple mathematical manipulation of Eqs (8) and (9), and using the operators defined in Eq. (7), one can show that the displacement components can be expressed in terms of generalized strain components as:

$$\nabla_1^2u=\frac{\partial\Delta}{\partial r}+\frac{\partial\mho_\theta}{\partial z} \tag{10}$$

$$\nabla_0^2 \omega = \frac{\partial \Delta}{\partial z} - \frac{1}{r}\frac{\partial (r \upsilon_\theta)}{\partial r} \tag{11}$$

In addition, stress-displacement relations can be expressed as:

$$\sigma_r = \lambda \Delta - 2\mu \frac{\partial u}{\partial r} \tag{12}$$

$$\sigma_z = \mu \frac{\partial u}{\partial z} + \mu \frac{\partial \omega}{\partial r} \tag{13}$$

where σ_r and σ_z are the radial and axial components of stress.

3 WAVELET-BASED DAUBECHIES

In this section, the wavelet-based finite element (WBFE) method as the main approach for the crack detection procedure is employed using Daubechies wavelet family as mother wavelet function. Mother wavelets that are the basis of wavelets are of the form $\psi_{j,k}(t)$. As it is a pivotal requirement for all functions prior to the qualification as basis for a particular space, they are orthogonal and span the L^2 space corresponding to the set of values chosen from $|R$.

Each wavelet has two defining components that are scaling and shifting characteristics with specific notations as $\varphi(t)$ and $\psi(t)$ related to the scale and mother functions, respectively. Their implicit form of function can be presented as:

$$\varphi(t) = \sum_k a_k \varphi(2t - k) \tag{14}$$

$$\psi(t) = \sum_k (-1)^k a_{1-k} \varphi(2t - k) \tag{15}$$

where the coefficient a_k is regarded as the wavelet filter coefficient which is specific to each wavelet and its particular scale value.

3.1 Time estimation

The first step in the WBFE formulation is the simplification of equations of motion, namely Eqs. (2) and (5). In this regard, the generalized strains Δ, υ_θ and partial differential operators ∇_n^2 $(n = 0,1)$ are introduced to the wavelet domain based on the discretization of time domain with respect to the orthogonal wavelet basis.

Dividing the function $\Delta(r,z,t)$ to n points within $[0,t_f]$ time and noting that $\tau = 0,1,2,...,n-1$ are arbitrary sampling points, one can write

$$t = \Delta(t)\tau \tag{16}$$

where $\Delta(t)$ is time between two sampling points.

In addition, $\Delta(r,z,t)$ can be approximated using the wavelet function $\varphi(t)$ in an arbitrary scale such that

$$\Delta(r,z,t) = \Delta(r,z,\tau) = \sum_k \Delta_k(r,z)\varphi(\tau - k) \tag{17}$$

In which k belongs to the set of real numbers, namely $|Z$.

For convenience, from now on Δ_k will be used instead of $\Delta_k(r,z)$ with the same meaning. Therefore, introducing Eq. (17) into Eq. (2), gives

$$\sum_k c_d^2\left(\frac{\partial^2}{\partial r^2}+\frac{1}{r}\frac{\partial}{\partial r}+\frac{\partial^2}{\partial z^2}\right)\Delta_k\varphi(\tau-k)=\frac{1}{\Delta t^2}\sum_k\Delta_k\varphi''(\tau-k) \tag{18}$$

It should be noted that the scale operator $\varphi(\tau-k)$ is appeared in both sides of the Eq. (18). Making use of the orthogonality of wavelet functions and knowing the fact that Eq. (18) can be treated separately as n partial differential equations (PDEs), one can show that

$$c_d^2\left(\frac{\partial^2}{\partial r^2}+\frac{1}{r}\frac{\partial}{\partial r}+\frac{\partial^2}{\partial z^2}\right)\Delta_j=\frac{1}{\Delta t^2}\sum_{k=j-N+2}^{j+N-2}\Omega_{j-k}^2\Delta_k \tag{19}$$

where $j=0,1,2,...,n-1$, N is the order number of Daubechies wavelet, and Ω_{j-k}^2 is the connection coefficient of second degree which can be calculated from

$$\Omega_{j-k}^2=\int\varphi''(\tau-k)\varphi(\tau-j)d\tau \tag{20}$$

In a similar manner, the following equation is valid for the connection coefficient of first degree, that is Ω_{j-k}^1

$$\Omega_{j-k}^1=\int\varphi'(\tau-k)\varphi(\tau-j)d\tau \tag{21}$$

For this compact wavelet type, Ω_{j-k}^1 and Ω_{j-k}^2 in the range of $k=j-N+2$ to $k=j+N-2$ are always nonzero [18]. Examining Eq. (19), one can simply verify that it is a possibility for the coefficient of Δ_j in some cases to be out of time period range $[0,t_f]$, namely when $j=0$ or $j=n-1$. These coefficients have to be checked and analyzed using finite element method within finite domain properly [19]. In the present work, an extrapolation wavelet-based method is used in order to address the issue of boundary points.

Eq. (19) can be further simplified as follows:

$$c_d^2\left(\frac{\partial^2}{\partial r^2}+\frac{1}{r}\frac{\partial}{\partial r}+\frac{\partial^2}{\partial z^2}\right)\{\Delta_j\}=[\Gamma^1]\{\Delta_j\} \tag{22}$$

where $[\Gamma^1]$ is the first order connection coefficient matrix and it can be calculated based on wavelet-based extrapolation. Using the eigenvalue analysis, the aforementioned set of PDEs can be separated as follows:

$$\Gamma^1=\Phi\Pi\Phi^{-1} \tag{23}$$

where Π is diagonal matrix containing eigenvalues and Φ is the eigenvector matrix of $[\Gamma^1]$. It can be shown that eigenvectors have the form $i\gamma_j$ where $i=\sqrt{-1}$.

Accordingly, PDEs related to the Eq. (22) can be presented separately as:

$$c_d^2\left(\frac{\partial^2}{\partial r^2}+\frac{1}{r}\frac{\partial}{\partial r}+\frac{\partial^2}{\partial z^2}\right)\hat{\Delta}_j=-\gamma_j^2\hat{\Delta}_j \tag{24}$$

where $\hat{\Delta}_j$ can be calculated as:

$$\hat{\Delta}_j = \Phi^{-1}\Delta_j \tag{25}$$

Performing the similar procedure described in this section on Eq. (5) results in the following final modified form of PDEs

$$c_s^2(\frac{\partial^2}{\partial r^2}+\frac{1}{r}\frac{\partial}{\partial r}-\frac{1}{r^2}+\frac{\partial^2}{\partial z^2})\hat{\upsilon}_{\theta j} = -\gamma_j^2\hat{\upsilon}_{\theta j} \tag{26}$$

where as mentioned earlier in this section $j = 0,1,2,...,n-1$.

In addition, final modified form of Eqs. (10-13) can be rewritten as follows:

$$\nabla_1^2\hat{u}_j = \frac{\partial\hat{\Delta}_j}{\partial r}+\frac{\partial\hat{\upsilon}_{\theta j}}{\partial z} \tag{27}$$

$$\nabla_0^2\hat{w}_j = \frac{\partial\hat{\Delta}_j}{\partial z}-\frac{1}{r}\frac{\partial(r\hat{\upsilon}_{\theta j})}{\partial r} \tag{28}$$

$$\hat{\sigma}_{rj} = \lambda\hat{\Delta}_j + 2\mu\frac{\partial\hat{u}_j}{\partial r} \tag{29}$$

$$\hat{\sigma}_{zj} = \mu\frac{\partial\hat{u}_j}{\partial z}+\frac{\partial\hat{\omega}_j}{\partial r} \tag{30}$$

where the superscript ^ indicates the modified form of variables in Eqs. (26-30).

3.2 Spatial estimation

Using the same procedure mentioned in subsection 3.1, transformed variable $\hat{\Delta}_j$ can be further discretized in the spatial domain $[0, L_z]$ to *n* points, where L_z is the length in the *z* direction.

In this subsection sampling points denoted by $\xi = 0,1,2,...,m-1$ are related to the spatial variable such that

$$z = \Delta z\,\xi \tag{31}$$

where Δz is the interval between two sampling points.

Similar to the Eq. (17) in the previous subsection, $\hat{\Delta}_j(r,z)$ can be introduced into the wavelet space as follows:

$$\hat{\Delta}_j(r,z) = \hat{\Delta}_j(r,\xi) = \sum_l \hat{\Delta}_{lj}(r)\varphi(\xi-l) \tag{32}$$

In which *l*, as shifting parameter, belongs to the set of real numbers, namely $|Z$.

Applying the wavelet transformation presented in Eq. (32), one can rewrite Eq. (24) as follows:

$$c_d^2(\frac{d^2}{dr^2}+\frac{1}{r}\frac{d}{dr})\hat{\Delta}_{lj}\varphi(\xi-l)+c_d^2\frac{1}{\Delta z^2}\hat{\Delta}_{lj}\varphi''(\xi-l) = -\gamma_j^2\hat{\Delta}_{lj}\varphi(\xi-l) \tag{33}$$

Invoking the orthogonality condition of wavelet functions, one can rewrite Eq. (33) in terms of the connection coefficients knowing $l = 0,1,2,...,m-1$ as follows:

$$c_d^2(\frac{d^2}{dr^2}+\frac{1}{r}\frac{d}{dr})\hat{\Delta}_{lj}+c_d^2\frac{1}{\Delta z^2}\sum_{l=i-N+2}^{i+N-2}\hat{\Delta}_{lj}\,\Omega_{i-1}^2=-\gamma_j^2\hat{\Delta}_{lj} \tag{34}$$

where N is the order number of Daubechies wavelet.

In this equation some coefficients in the vicinity of the boundary, namely $i=0$ or $i=m-1$, which are not in the range $[0,L_z]$ can be analyzed using extrapolation technique as mentioned in the previous subsection. It should be noted that for the fixed-free boundary condition presenting the formulations using the matrix notation is a suitable approach. In addition, incorporating it in the numerical wavelet-based finite element method is a straightforward way of presenting the concepts.

Now after determining the unknown coefficients that are out of time and spatial domains, due to the boundary condition, internal coefficients can be rewritten as follows:

$$c_d^2(\frac{d^2}{dr^2}+\frac{1}{r}\frac{d}{dr})\{\hat{\Delta}_{ij}\}+c_d^2[\Lambda^1]\{\hat{\Delta}_{ij}\}=-\gamma_j^2\{\hat{\Delta}_{ij}\} \tag{35}$$

where $[\Lambda^1]$ is the first order coefficient of connection matrix and can be expressed as:

$$[\Lambda^1]=\frac{1}{\Delta Y}\begin{bmatrix}\Omega_0^1 & \Omega_{-1}^1 & \dots & \Omega_{-N+2}^1 & \dots & \Omega_{N-2}^1 & \dots & \Omega_1^1\\ \Omega_1^1 & \Omega_0^1 & \dots & \Omega_{-N+3}^1 & \dots & 0 & \dots & \Omega_2^1\\ \vdots & \vdots & & \vdots & & \vdots & & \vdots\\ \Omega_{-1}^1 & \Omega_{-2}^1 & \dots & 0 & \dots & \Omega_{N-3}^1 & \dots & \Omega_0^1\end{bmatrix} \tag{36}$$

where ΔY is a constant.

Denoting eigenvalues by $i\beta_i$ where $i=\sqrt{-1}$, Eq. (35) can be further simplified as:

$$c_d^2(\frac{d^2}{dr^2}+\frac{1}{r}\frac{d}{dr}-\beta_i^2)\tilde{\Delta}_{ij}=-\gamma_j^2\tilde{\Delta}_{ij} \tag{37}$$

where the superscript $\sim$ indicates the second modification (spatial modification) of variables.

Performing the similar procedure of spatial modification presented in this section on Eq. (26) results in the final form

$$c_s^2(\frac{d^2}{dr^2}+\frac{1}{r}\frac{d}{dr}-\frac{1}{r^2}-\beta_i^2)\tilde{\upsilon}_{\theta ij}=-\gamma_j^2\tilde{\upsilon}_{\theta ij} \tag{38}$$

Similarly, introducing spatial transformations into Eqs. (27-30), one can rewrite them as follows:

$$(\frac{d^2}{dr^2}+\frac{1}{r}\frac{d}{dr}-\frac{1}{r^2}-\beta_i^2)\,\tilde{u}_{ij}=\frac{d\tilde{\Delta}_{ij}}{dr}-i\beta\tilde{\upsilon}_{\theta ij} \tag{39}$$

$$(\frac{d^2}{dr^2}+\frac{1}{r}\frac{d}{dr}-\beta_i^2)\tilde{\omega}_{ij}=-i\beta_i\tilde{\Delta}_{ij}-\frac{1}{r}\frac{d(r\tilde{\upsilon}_{\theta ij})}{dr} \tag{40}$$

$$\tilde{\sigma}_{rij}=\lambda\tilde{\Delta}_{ij}+2\mu\frac{d\tilde{u}_{ij}}{dr} \tag{41}$$

$$\tilde{\sigma}_{zij}=-i\beta_i\mu\tilde{u}_{ij}+\frac{d\tilde{\omega}_{ij}}{dr} \tag{42}$$

3.3 Wavelet calculation

The obtained equations in the previous subsection have coefficients similar to the governing equations of the beams and plates. These coefficients are functions of radius *r*.

In order to solve Eqs. (37-42) for any desired transformed variable, one can assume that the solution of $\tilde{u}_{ij}$ and $\tilde{\omega}_{ij}$ to be of the form

$$\tilde{u}_{ij} = \sum_{k=1}^{6} \bar{u}_{ij} e^{-ikr} \tag{43}$$

$$\tilde{\omega}_{ij} = \sum_{k=1}^{6} \bar{\omega}_{ij} e^{-ikr} \tag{44}$$

where *k* is the wavelet number in the direction of *r*.

Substituting Eqs (43) and (44) in Eqs (37) and (38), one can show that the resulting equations can be expressed as:

$$\begin{aligned}&(ic_d^2 k^3 - (2c_d^2 k^2 / r) + i(\beta^2 c_d^2 - c_d^2 / r - \gamma^2)k + (-3c_d^2 / r^3 - c_d^2 \beta^2 / r + \gamma^2 / r))\bar{u} \\ &+(-ic_d^2 \beta k^2 + (c_d^2 \beta / r)\mathrm{k} + (\mathrm{i}c_d^2 \beta^3 - i\beta\gamma^2))\bar{\omega} = 0\end{aligned} \tag{45}$$

$$(-ic_s^2 \beta k^2 + (-c_s^2 \beta / r)\mathrm{k} - i(c_s^2 / r^2 - c_s^2 \beta^2 + \gamma^2)\beta)k + (-ic_s^2 \mathrm{k}^3 + (c_s^2 / r)\mathrm{k}^2 - \mathrm{i}(c_s^2 / r + c_s^2 \beta^2 - \gamma^2)\mathrm{k})\bar{\omega} = 0 \tag{46}$$

where the above equations can be solved to obtain wavelet-based number *k* for any specific range.

These equations are solved using polynomial eigenvalue method similar to the Chakraborty and Gopalakrishnan [20]. Eigenvalue equations can be expressed in the form

$$\mathbf{A}_3 k^3 + \mathbf{A}_2 k^2 + \mathbf{A}_1 k + \mathbf{A}_0 = 0 \tag{47}$$

where A_1, A_2, A_3, A_4 are the 2×2 matrices obtained from the WBFE which are the exact fractions of Nyquist frequencies (f_{nyq}). This fraction which is denoted by p_N , is dependent on the Daubechies wavelet order number *N*.

4 RESULTS AND DISCUSSION

In this section, in order to perform the numerical analysis, a pressure vessel model with fixed ends at the bottom of the supporting legs is created in the Abaqus software. Dimensions, Geometrical features, and mechanical properties as well as pressure forces are the same for all cases of the analysis. The material properties required for the analysis are those of steel with the Young's modulus of $2.1 \times 10^6 \, (kg/cm^2)$ and Poisson's ratio of 0.29. In addition, with respect to the linear elastic assumption for displacement response of the pressure vessel, the internal pressure has a value of 5 (*bar*). The length of the vessel where the cracks are located is 1000 (*mm*) with the internal radius 350(*mm*) and the external one 500(*mm*). Furthermore, the cracks have the length of 1(*mm*) and the depth of 20(*mm*), which after the mesh generation can be shown as depicted in Fig. 1.

Based on the results from the pressure vessel model, there are different displacement components in each direction of the coordinate system. The total magnitude of these components in the case of intact vessel is depicted in Fig. 1 that also includes the geometry of the vessel without mesh using Abaqus software.

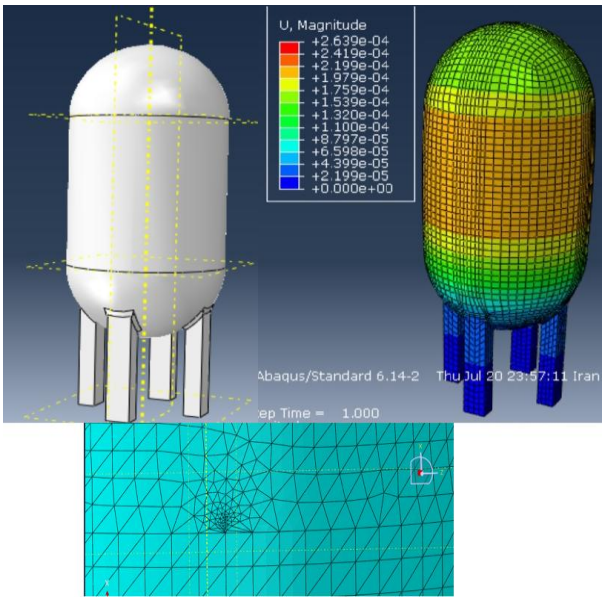

Fig.1
From the top left to the bottom: Geometry of the pressure vessel, displacement results in the intact pressure vessel, and mesh generation results in the vicinity of the crack.

The next step is introducing cracks in the length direction of the vessel, and then evaluating the displacement field across different paths including elements and their intersections on the outer curvilinear edges of the pressure vessel. This time the results for the two components of displacement across the vessel with a crack are shown in Fig. 2 that can be used together with the same data obtained from the case without crack for further numerical analysis as mentioned earlier in the previous section.

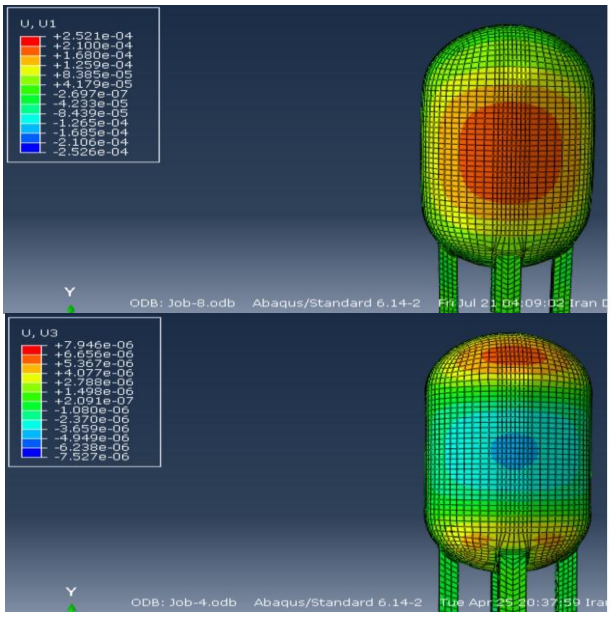

Fig.2
The results of evaluations of displacement components in the length (top picture) and thickness (bottom picture) directions in the vessel with a crack.

Finally, the displacement data is gathered using different paths and transferred to Matlab software for the wavelet analysis.

Fig. 3 shows the results for wavelet analysis based on continuous scale range from 1 to 64 for the vessel without crack. For this purpose a wavelet function of Daubechies 4 is used which is a built-in wavelet function of Matlab software as well. As expected, no crack is detected in the small-scale numbers that are highly sensitive to any changes in the mechanical response of the structure. However, with increasing the scale numbers the discontinuity resulting from the sudden changes related to the very ends of the results has more dominating effect near the end locations where data is not available beyond those boundaries.

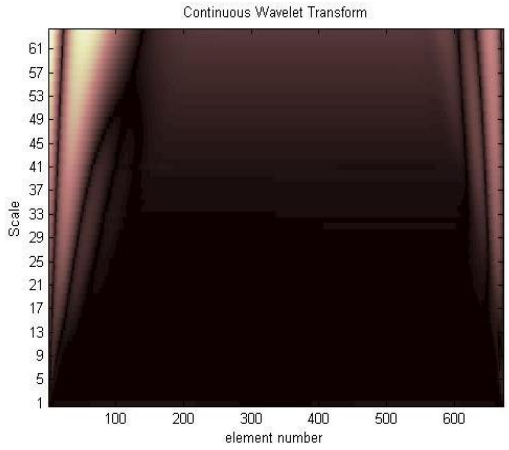

Fig.3
Wavelet analysis of the results for the intact vessel including a continuous wide range of scales from 1 to 64.

In order to further, illustrate the arguments made in the previous paragraph, The discrete results for small scale numbers for the wavelet analysis of intact vessel by Daubechies 4 is depicted in Fig. 4 which, again, confirms that no alteration is detected in the results regarding to the crack presence.

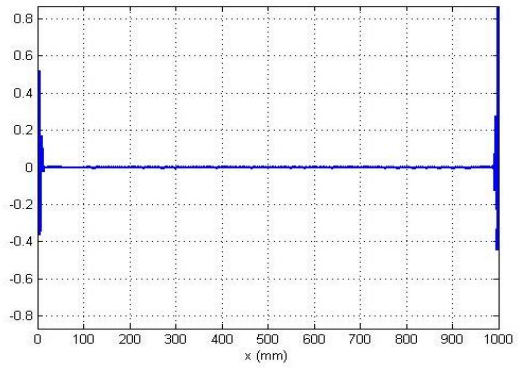

Fig.4
Daubechies wavelet analysis of intact pressure vessel.

The following Figure (Fig. 5) in which the maximum points of compression coefficients are evaluated shows the locations where the maximum similarity occur between the rough curves of the wavelet function and the mechanical response curve. The importance of these results lies within the comparison between the intact and damaged cases.

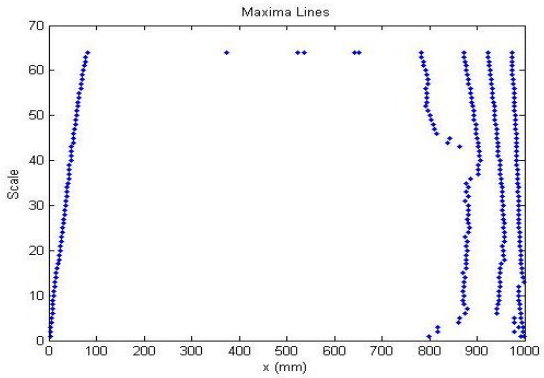

Fig.5
The maximum points of compressions in the intact vessel.

Incorporating the results for the model with a crack at 200 (*mm*) and performing the same procedure as explained for the model without crack, the resulting numerical data can be depicted as shown in Figs. 6-7.

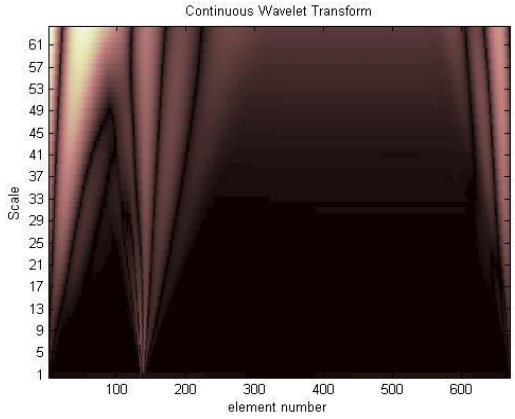

Fig.6
Wavelet analysis of the results for the vessel with a crack at 200 (mm) including a continuous wide range of scales from 1 to 64.

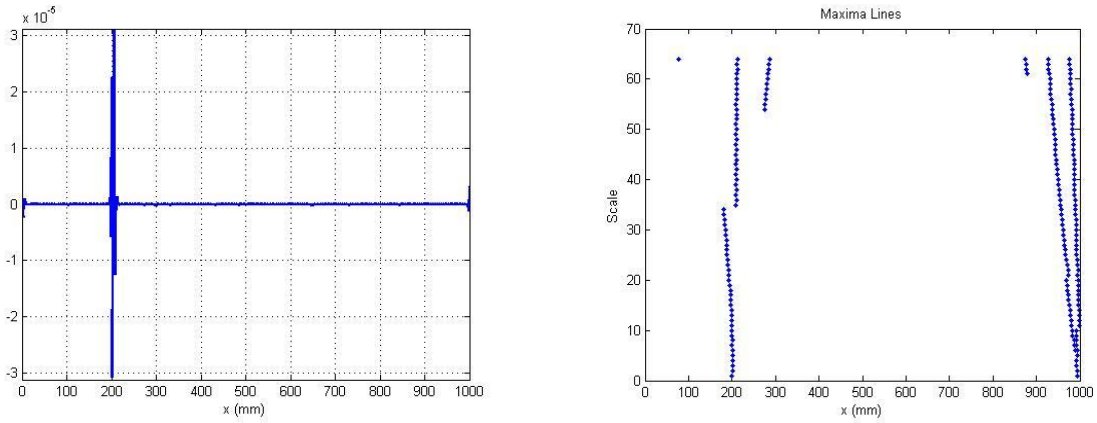

Fig.7
Wavelet analysis results for the vessel with a crack at 200 (*mm*) which can be compared to the results of Figs. 4-5 obtained for the intact vessel (The left picture corresponds to small scale wavelet analysis while the right one depicts the Maxima lines for a wide range of scales from 1 to 64 related to the maximum points of compressions).

Using these results Figs. 6-7 and comparing them with the intact case, it is clear that the crack and its location is predicted accurately by wavelet analysis. As mentioned earlier in this section, it is suitable to use lower scales since they give more accurate results in terms of prediction of the crack location; however, as it can be seen from Figs. 3-6, the analysis results can be directly presented for any scale number. Now in order to present the results for higher scale numbers, scale number 30 is chosen and its results are shown in Fig. 8.

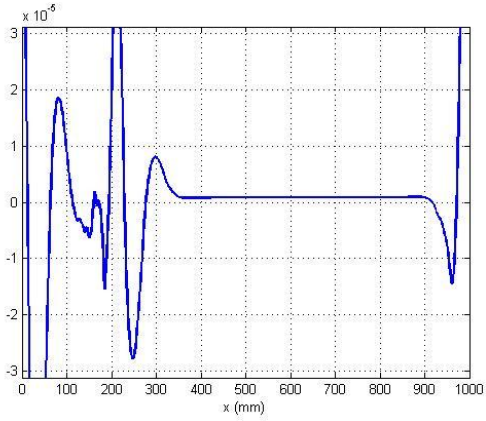

Fig.8
Curve with the scale number 30 from wavelet analysis of the pressure vessel with a crack at 200 (*mm*).

As the results suggest, at the higher scales the results can be useful for the determination of the approximate range of the crack location and cannot be used to verify the exact location. All of the aforementioned process can be repeated for a crack located at 400 (*mm*) which gives the following results Fig. 9 and 10.

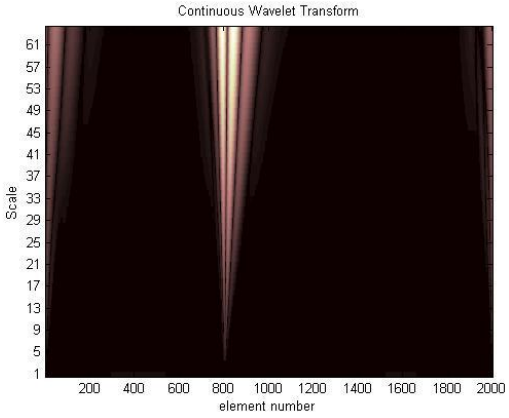

Fig.9
Continuous wavelet transform of the results for the vessel with a crack at 400 (*mm*) including a continuous range of scales.

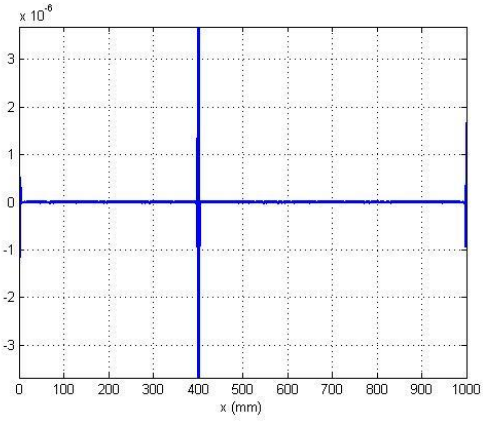

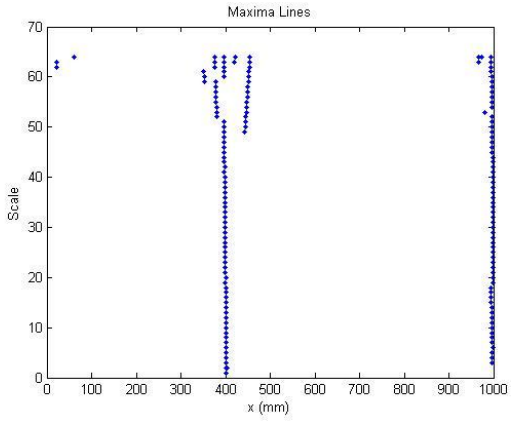

Fig.10
Wavelet analysis results for the vessel with a crack at 400 (*mm*) which can be compared to the results of Figs. 4-5-7.

It can be seen that the crack at 400 (*mm*) is properly detected in the above Figs. 9-10. As the results show, the crack in the length direction of the vessel can be detected very effectively using wavelet-based finite element method. By comparing the intact vessel results to those of the vessel with crack, one can easily locate the crack by noting the alterations in the behavior of numerical charts that is a suitable and more importantly a nondestructive method for detecting cracks. Moreover, the same results can be obtained for other directions in the vessel as it can be seen in the following Figure from the analysis data of the vessel with crack located at r=470 (*mm*), Fig. 11.

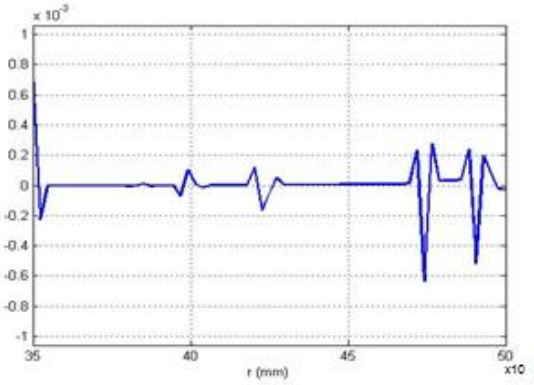

Fig.11
Daubechies wavelet analysis of the pressure vessel with crack located at r=470 (*mm*).

The same procedure can be performed using Haar wavelet type in which the results indicate no alteration in the location of the cracks. It is clear that there are no difference between analysis of the vessel in the presence or absence of the crack in the case of employing Haar wavelet. Therefore, Haar wavelet is unable to give any information regarding the presence of the crack or its location. In addition, in order to further illustrate the capabilities of powerful algorithm for crack detection presented in this work, the cracks located in the circumferential direction of the vessel were analyzed. The results of continuous wavelet analysis, maximum points of compressions, and small-scale analysis are shown in Figs. 12-14, respectively. The crack is successfully located and the presented algorithm properly magnified the small perturbation in the deflection curve caused by a crack at 245^0 with respect to the origin of circumferential coordinate.

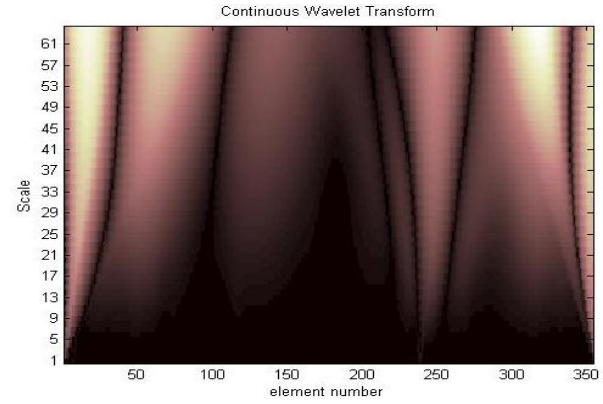

Fig.12
Continuous wavelet transform of the results for the vessel with a crack at 245^0 including a continuous range of scales.

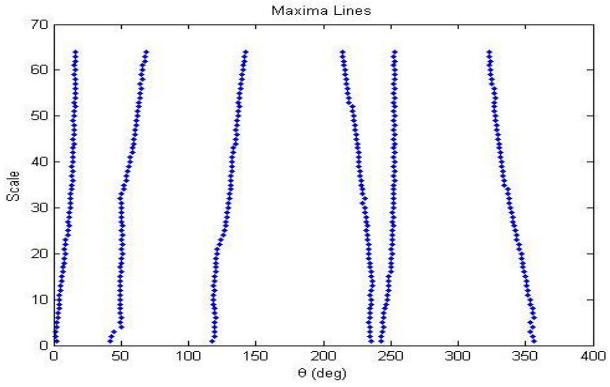

Fig.13
The maximum points of compressions for the vessel with a crack at 245^0.

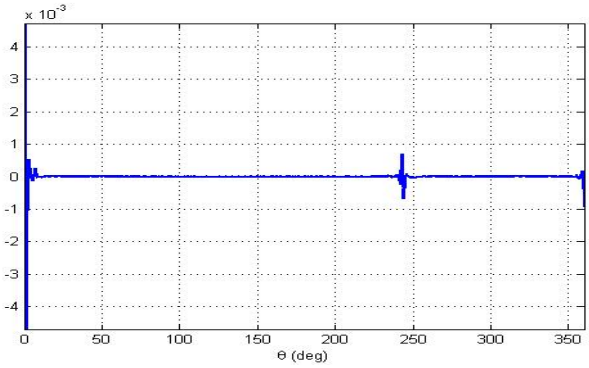

Fig.14
Daubechies wavelet small-scale analysis of the vessel the vessel with a crack at 245^0.

5 CONCLUSION

Crack location can be located by comparison between the intact and damaged vessels noting that the behavior of the analysis diagram alters in the crack location. Thus, wavelet-based finite element method, which is presented as an

integrated algorithm in this work, is a powerful tool and a numerical approach for the crack detection. It should be noted that this method is defined as a nondestructive way for detecting the cracks and other types of discontinuities in the structures. As the results suggest, a powerful wavelet type for this purpose is the Daubechies wavelet family. As it is mentioned in the paper, using the scale and transfer properties in the proper wavelet functions, any type of damage and discontinuity can be located in the structures. Another important investigation in this study is the comparison of the results based on the types of wavelet functions used in the analysis. For this purpose, two wavelet functions including Daubechies wavelet family and the Haar wavelet were used. The results showed that the latter proved to be not useful for the detection of crack in this study indicating that the selection of the wavelet function is of crucial importance in order to achieve the accurate results.

REFERENCES

[1] Gudmaunson P., 1982, Engine frequency changes of structures due to cracks, notches or other geometrical changes, *Journal of Mechanics and Physics of Solids* **30**: 339-353.

[2] Banks H.T., Inman D.J., Leo D.J., Wang Y., 1996, An experimentally validated damage detection theory in smart structures, *Journal of Sound and Vibration* **191**: 859-880.

[3] Ku C.J., Cermak J.E., Chou L.S., 2007, Random decrement based method for modal parameter identification of a dynamic system using acceleration responses, *Journal of Wind Engineering and Industrial Aerodynamics* **95**: 389-410.

[4] Li B., Chen X.F., Ma J.X., He Z.J., 2004, Detection of crack location and size in structures using Wavelet finite element methods, *Journal of Sound and Vibration* **285**: 767-782.

[5] Samii A., Lotfi V., 2007, Comparison of coupled and decoupled modal approaches seismic analysis of concretegravity damsin timedomain, *Finite Elements in Analysis and Design* **43**: 1003-1012.

[6] Douka E., Loutridis S., Trochidis A., 2003, Crack identificationin beams using Wavelet analysis, *International Journal of Solids and Structures* **40**: 3557-3569.

[7] Bagheri A., Ghodrati Amiri G., Khorasani M., 2010, Structural damage identification of plates based on modal data using 2D discrete Wavelet transform, *Journal of Structural Engineering and Mechanics* **40**: 13-28.

[8] Bagheri A., Ghodrati Amiri G., Seyed Razzaghi S.A., 2009, Vibration-based damage identification of plate structures via curvelet transform, *Journal of Sound and Vibration* **327**: 593-603.

[9] Rizos P.F., Aspragathos N., Dimaroginas A.D., 1990, Identification of crack location and magnitude in Cantilever beam from the vibration modes, *Journal of Sound and Vibration* **138**: 381-388.

[10] Melhem H., Kim H., 2003, Damage detection in concrete by Fourier and Wavelet analyses, *Journal of Engineering Mechanics* **129**: 571-577.

[11] Ovanesova A.V., Suarez L.E., 2004, Applications of Wavelet transforms to damage detection in frame structures, *Journal of Engineering Structure* **26**: 39-49.

[12] Khatam H., Golafshani A.A., 2004, Damage detection in beam using Wavelet transform, M.Sc. Dissertation, Sharif University of Technology.

[13] Cawely p., Adams R.D., 1979, Defect location in structures by a vibration technique, *American Society of Mechanical Engineering Technical Conference*, Louis.

[14] Gokdag H., Kopmaz O., 2009, A new damage detection approach for beam-type structures based on the combination of continuous and discrete Wavelet transforms, *Journal of Sound and Vibration* **324**: 1158-1180.

[15] Rucka M., 2011, Damage detection in beams using Wavelet transform on higher vibration modes, *Journal of Theoretical and Applied Mechanics* **49**: 399-417.

[16] Tao C., Fu Y., Dai T., 2017, Dynamic analysis for cracked fiber-metal laminated beams carrying moving loads and its application for wavelet based crack detection, *Composite Structures* **1**(159): 463-470.

[17] Mardasi A.G., Wu N., Wu C., 2018, Experimental study on the crack detection with optimized spatial wavelet analysis and windowing, *Mechanical Systems and Signal Processing* **1**(104): 619-630.

[18] Williams J.R., Amaratunga K., 1997, A discrete wavelet transform without edge effects using wavelet extrapolation, *Journal of Analysis Fourier and Applications* **3**(4): 435-449.

[19] Beylkin G., 1992, On the representation of operators in bases of compactly supported wavelets, *SIAM Journal on Numerical Analysis* **29**(6): 1716-1740.

[20] Chakraborty A., Gopalakrishnan S., 2005, A spectrally formulated plate element for wave propagation analysis in anisotropic material, *Computer Methods Applied Mechanics and Engineering* **194**: 42-44.